Available online at www.sciencedirect.com
SCIENCE DIRECT®

Microporous and Mesoporous Materials 69 (2004) 43–48

MICROPOROUS AND MESOPOROUS MATERIALS

www.elsevier.com/locate/micromeso

Room temperature synthesis of ordered porous silicas templated by symmetric and dissymmetric gemini surfactants $[C_nH_{2n+1}N(CH_3)_2(CH_2)_2(CH_3)_2NC_mH_{2m+1}]Br_2$

Francisco J. Romero [a,*], César Jiménez [a], Ivan Huc [b], Reiko Oda [b]

[a] Department of Organic Chemistry, Faculty of Sciences, University of Córdoba, Campus de Rabanales, Edificio Marie-Curie, Ctra. Nnal. IV, km 396, 14014 Córdoba, Spain
[b] Institut Européen de Chimie et Biologie, 16 Av. Pey Berland, 33607 Pessac Cedex, France

Received 17 December 2003; received in revised form 17 December 2003; accepted 31 January 2004

Abstract

Cubic and hexagonal ordered porous silicas can be synthesized under acidic or alkaline conditions at room temperature by using symmetric (10–2–10 and 12–2–12) and dissymmetric (8–2–16) gemini surfactants as templates. Among others, high-quality MCM-41 and MCM-48 materials were obtained. These materials exhibited high specific surface areas and pores with sizes in between the micro and meso ranges. The results obtained have been related to the structural features of the surfactants as well as to the synthesis conditions.

© 2004 Elsevier Inc. All rights reserved.

Keywords: Mesoporous silica; Templated synthesis; Gemini surfactants; Mesophases; MCM-41; MCM-48

1. Introduction

The synthesis of mesoporous solids has aroused vast interest because of their potential applications as catalysts [1], optical and conducting materials [2], etc. These solids are synthesized using surfactant assemblies as templates, thus ensuring the formation of ordered mesostructured materials [3–5]. These processes were initially conducted with cationic [3] and later with anionic [6] and neutral [7] surfactants.

Gemini surfactants $[C_nH_{2n+1}N(CH_3)_2(CH_2)_s(CH_3)_2NC_mH_{2m+1}]Br_2$ are two-chain dicationic surfactants, which are denoted as *n*–*s*–*m*, where *n* and *m* refer to the length of the alkyl tails and *s* is the number of methylene units of the alkyl spacer. Some of them have been used for the synthesis of molecular sieve materials [6]. Assemblies of divalent quaternary ammonium surfactant *n*–*s*–1 resulted in the formation of a regular caged mesoporous silicate with hexagonal symmetry, SBA-2, under both acid and basic conditions, whereas 12–12–12 and 16–12–16 gave hexagonal (MCM-41) and cubic (MCM-48) phases, respectively [8]. Under basic conditions, surfactants 16–*s*–16 ($s = 2$–12) yielded a variety of phases. Thus, a small *s* favoured the formation of a lamellar phase (MCM-50), whereas larger *s* provided MCM-41 [9]. The hexagonal phase SBA-3 was obtained with the same surfactants in acidic media.

The drawbacks and poor reproducibility in the synthesis of MCM-48, which possesses a high potential as adsorbent and catalytic support, have favoured the use of some of these gemini surfactants in order to obtain good-quality materials [10–12]. Also, gemini surfactants *n*–3–1 (particularly, those with $s = 16$, 18) have been shown to be suitable templates for the synthesis of the three-dimensional hexagonal (SBA-2) and cubic (SBA-1) mesoporous silicas [13–16].

Recently, it has been reported that gemini surfactants with $s = 2$ display a great variety of phases in water depending both on chain length and chain length difference (dissymmetry) [17,18]. New applications of these compounds are being envisaged, such as low molecular weight gelators [19] or as templates (with chiral

---

* Corresponding author. Tel.: +34-957-212-065; fax: +34-957-212-066.
E-mail addresses: qo2rosaf@uco.es (F.J. Romero), ivan.huc@iecb-polytechnique.u-bordeaux.fr (I. Huc).

1387-1811/$ - see front matter © 2004 Elsevier Inc. All rights reserved.
doi:10.1016/j.micromeso.2004.01.005

counterions) for the synthesis of double helical silica fibrils by sol–gel transcription [20].

This paper reports the synthesis of ordered porous silicas under acidic or basic conditions by use of three surfactants of the *n*–2–*m* series as structure-directing agents: two symmetric (12–2–12 and 10–2–10) and one dissymmetric (8–2–16) gemini surfactants possessing the same overall hydrocarbon content as 12–2–12 (same $m + n$).

2. Experimental

Gemini surfactants were synthesized as previously described [18]. The critical micelle concentrations (cmc) for *n*–2–*m* gemini surfactants are close to a linear function of chain length, being very similar for surfactants with the same $n + m$. The cmc for surfactants 12–2–12 and 8–2–16 are 9.5×10^{-4} and 7.8×10^{-4} M, respectively, whereas for surfactant 10–2–10 should be around 4×10^{-3} M.

All silicas were prepared following a similar procedure. Thus, a surfactant solution, under stirring, was supplied with the acid (HCl) or base (NaOH). Then, tetraethoxysilane (TEOS) was added and stirring was continued for a further 30 min at room temperature. The mole proportions of the different components in the initial mixtures are indicated in Tables 1 and 2. The resulting suspension was allowed to stand for either 1 or 24 h and the precipitate was filtered, washed with distilled water and air-dried. Finally, the solid was heated in the air at 1 °C min^{-1} up to 600 °C, which was held for 3 h.

X-ray diffractions patterns were recorded on a Siemens D5000 diffractometer using CuKα radiation. N_2 isotherms were determined on a Micromeritics ASAP 2000 analyzer. The specific surface area of each solid was determined using the BET method.

3. Results and discussion

Mesoporous silicates are synthesized by following different synthesis routes, which depend on the various types of inorganic-surfactant head group interactions [21]. In our case, the formation of the different materials is based on the electrostatic interaction between an inorganic precursor (I) and the cationic head group of the gemini surfactants (S^+). Two charge-interaction pathways are possible: S^+I^- and $S^+X^-I^+$ (X^- being a counteranion), under basic and acidic conditions, respectively.

Under acidic conditions, XRD patterns indicated that all surfactants gave hexagonal ordered silicas after 24 h (Table 1). Those materials synthesized in the presence of symmetric surfactants, 12–2–12 (**2**) and 10–2–10 (**3**), exhibited a low angle peak (1 0 0), with a d-spacing of 33.0 and 30.8 Å, respectively. However, the second-order peaks obtained at higher incidence angles were broad and short. The material templated by the surfactant 8–2–16 (**4**) displayed the (1 0 0) and (1 1 0) reflections at 34.2 and 19.8 Å, respectively (Fig. 1). According to the surfactant used, the unit cell dimension a ($2d_{100}/\sqrt{3}$) decreased in the order 8–2–16 > 12–2–12 > 10–2–10. A unit cell contraction was observed upon calcination (Table 1). Thermal treatment also produced a reduction of the order of the structure, losing the definition of the weaker XRD peaks. It should be noted that the higher quality of the 8–2–16 templated materials

Table 1
Physicochemical properties of the materials obtained under acidic conditions (surfactant/HCl/TEOS/H_2O molar ratio = 0.06/4.8/1/130)

Solid	Surfactant	Synthesis time (h)	Phase	*a* (as-synthesized) (Å)	*a* (calcined) (Å)	Surface area (*S*) (m^2 g^{-1})	Pore volume (*V*) (ml g^{-1})	Pore diameter[a] (*d*) (Å)	Pore wall thickness (Å)
1	12–2–12	1	Amorphous	–	–	696	1.08	55 (45)	–
2	12–2–12	24	Hexagonal	38.1	30.8	1340	0.63	20 (15)	11
3	10–2–10	24	Hexagonal	35.5	25.9	876	0.43	20 (12)	6
4	8–2–16	24	Hexagonal	39.5	33.9	1365	0.70	23 (17)	11

[a] The diameter of cylindrical pores was calculated as $d = 4V/S$. Values in brackets correspond to those determined by the BJH method.

Table 2
Physicochemical properties of the materials obtained under basic conditions (surfactant/NaOH/TEOS/H_2O molar ratio = 0.06/0.65/1/150)

Solid	Surfactant	Synthesis time (h)	Phase	*a* (as-synthesized) (Å)	*a* (calcined) (Å)	Surface area (*S*) (m^2 g^{-1})	Pore volume (*V*) (ml g^{-1})	Pore diameter[a] (*d*) (Å)	Pore wall thickness (Å)
5	12–2–12	1	Lamellar	–	–	412	0.21	39 (18)	–
6	12–2–12	24	Cubic	80.7	59.2	803	0.39	20 (13)	9
7	10–2–10	1	Hexagonal	33.1	27.1	569	0.29	20 (12)	7
8	8–2–16	1	Hexagonal	41.7	28.8	1022	0.50	19 (13)	10
9	8–2–16	24	Hexagonal	42.6	29.8	1023	0.50	19 (13)	11

[a] The diameter of cylindrical pores was calculated as $d = 4V/S$. Values in brackets correspond to those determined by the BJH method.

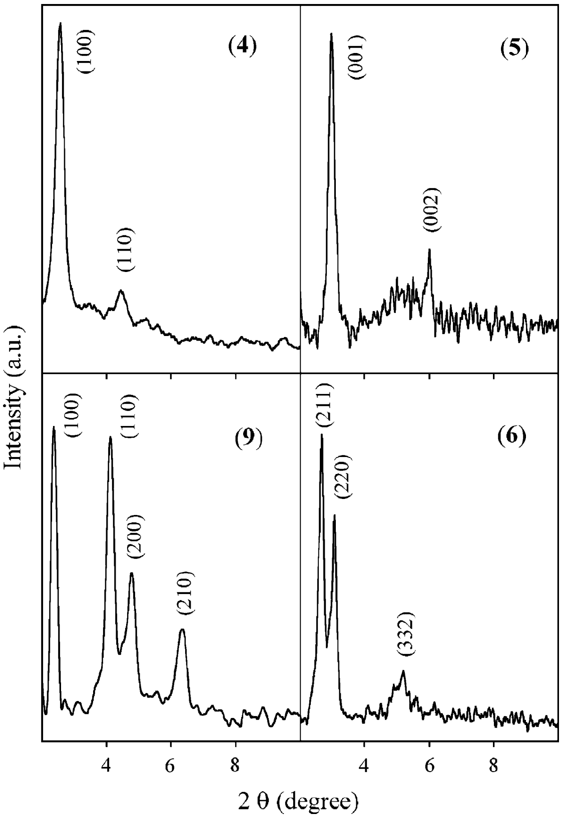

Fig. 1. Powder XRD patterns for some as-synthesized ordered silicas templated with gemini surfactants. Numbers in brackets correspond to those found in Tables 1 and 2.

(**4**) was also present after calcination and that of **3** was the poorest, with a rather broad low angle peak. Hexagonal mesophases (p6m), denoted as SBA-3, were also obtained by Huo et al. [9] from acidic synthesis media with gemini surfactants of the type 16–*s*–16 ($s = 3$–12).

The templated synthesis of silicas with these surfactants under basic conditions led to more ordered materials (Figs. 1 and 2). The alkalinity of the synthesis gel greatly influences the degree of silicate species condensation and so it leads to an improvement in the quality of the final material [22]. Interestingly, hexagonal phases were obtained with surfactants 10–2–10 and 8–2–16, but not with surfactant 12–2–12 (Table 2). The latter gave rise to a lamellar phase (**5**) after a synthesis time of 1 h. It displayed (0 0 1) and (0 0 2) reflections at 29.7 and 14.7 Å, respectively (Fig. 1). This phase collapsed upon calcination into an amorphous material. Increasing the synthesis time to 24 h, a highly ordered cubic phase was obtained (**6**). Its XRD pattern showed two intense peaks in the region $2\theta = 2$–4 corresponding to (2 1 1) and (2 2 0) reflections as well as a diffuse region resulting from (4 2 0), (3 3 2), (4 2 2) and (4 3 1) reflections, among others (Fig. 1), which is typical for MCM-48 (Ia3d). After calcination, only the (2 1 1) and (2 2 0) reflections were observed although the second one quite weak. The cubic unit cell parameter $a = d_{hkl} \cdot (h^2 + k^2 + l^2)^{1/2}$ is given in Table 2. On the other hand, surfactant 10–2–10 yielded a hexagonal phase (**7**) with the (1 0 0) and (1 1 0) reflections. After heating, only a broad peak corresponding to the (1 0 0) reflection remained. Also, dissymmetric surfactant 8–2–16 produced a hexagonal phase (**8** and **9**) but in this case of a high-quality, which exhibited the typical (1 0 0), (1 1 0), (2 0 0) and (2 1 0) reflections of MCM-41 (Figs. 1 and 2).

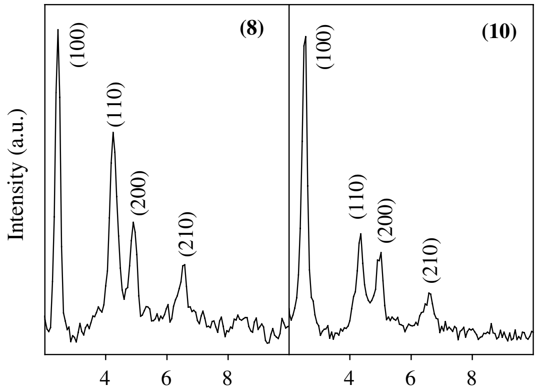

Fig. 2. Powder XRD patterns for solids **8** and **10** showing an MCM-41 mesophase. See Table 2 for captions. Material **10** was synthesized by an analogous procedure to that carried out for **9** but using a surfactant to silica ratio of 0.012 instead of 0.06.

The structure-directing effect of dissymmetric surfactant 8–2–16 for the hexagonal phase is so strong that, even when using a surfactant to silica ratio of 0.012 (with all other components in the same proportions relative to silica), materials of a similar quality to **4** and **9** were obtained in acidic and basic media, the latter one denoted as **10** (Fig. 2), respectively. A comparison revealed that the materials synthesized with a surfactant to silica ratio of 0.012 show a slightly lower distance between pore centers (a) than **4** and **9** (in acid: 36.6 compared to 39.5 Å for **4** and in base: 40.2 for **10** compared to 42.6 Å for **9**). Moreover, a 1:1 mixture of surfactants 12–2–12 and 8–2–16 (total surfactant to silica ratio of 0.06) in a basic medium gave MCM-41 with $a = 39.1$ Å. However, when using the surfactant 12–2–12 alone in a ratio of 0.012, the XRD pattern exhibited several overlapped low angle peaks with d-spacing between 34 and 29 Å, revealing the mixture of different phases. MCM-41 materials synthesized in the presence of dissymmetric gemini surfactant 8–2–16 under basic conditions, such as **8**, **9** and **10** (Figs. 1 and 2), exhibited very intense higher order reflections, particularly at higher surfactant to silica ratios, which could be ascribed to preferential orientations during the crystal growth.

Israelachvili et al. [23] and Stucky et al. [24] introduced the packing parameter, $g = V/a_o l$ (where V is the total volume occupied by the surfactant chain, a_o is the effective headgroup area at the micelle surface, and l is the kinetic length of the alkyl chain) to describe the tendency of an amphiphile to aggregate into a particular morphology. The packing parameter determines whether the amphiphile will form spherical micelles ($g < 1/3$), cylindrical micelles ($1/3 < g < 1/2$), vesicles or bilayers ($1/2 < g < 1$) or inverted structures ($g > 1$). At the surfactant concentrations used for the synthesis (1.2–1.5%), surfactants 8–2–16 and 10–2–10 mainly form spherical micelles, whereas surfactant 12–2–12 aggregates into entangled worm-like micelles. Both decreasing the chain length and dissymmetry cause an increase of the spontaneous curvature and therefore a decrease of the packing parameter [17].

The presence of a preorganized liquid crystal structure cannot be proposed under the synthesis conditions used. At present, it is accepted that the formation of the silica mesophases occurs via the cooperative charge density model [25,26]. In it, the surfactant is in equilibrium between spherical and cylindrical micelles on the one hand and isolated molecules on the other. Upon addition of the silica precursor, multicharged silicate species interact with charged surfactant molecules to form ion-pairs that associate in a new mesophase. The last step of the process would involve the polymerization and condensation of inorganic species.

The silicate-surfactant organization, which is governed by electrostatic interactions, is a determining factor in the formation of the different mesophases. These can be qualitatively predicted by the value of the surfactant packing parameter (g). The hexagonal mesophase forms for g-values below 0.5, the cubic mesophase (Ia3d) for g-values in the interval 0.5–0.65 and the lamellar phase for g-values above 0.65 [27,28]. When the silicate species involved are relatively small and highly charged, as for materials obtained under basic conditions, there are no essential differences between the general structural characteristics of silicate-surfactant systems and those of the surfactants themselves with simple counterions [28]. As a consequence, under basic conditions, surfactants 10–2–10 and 8–2–16 gave rise to hexagonal mesophases (solids **7**–**10**), whereas surfactant 12–2–12 yielded a cubic mesophase (solid **6**), as expected according to their g-values. The lamellar structure should require a higher charge density at the interfaces than a cubic one, which could explain the formation of solid **5** at a short synthesis time. On the other hand, at a low pH value (acidic conditions), the ion pairing interaction between the silicate and the surfactant head groups is changed due to a decrease in charge density of the inorganic region, thereby decreasing the surfactant packing parameter, even for surfactant 12–2–12, and redirecting the structure to a hexagonal mesophase (solids **2**–**4**).

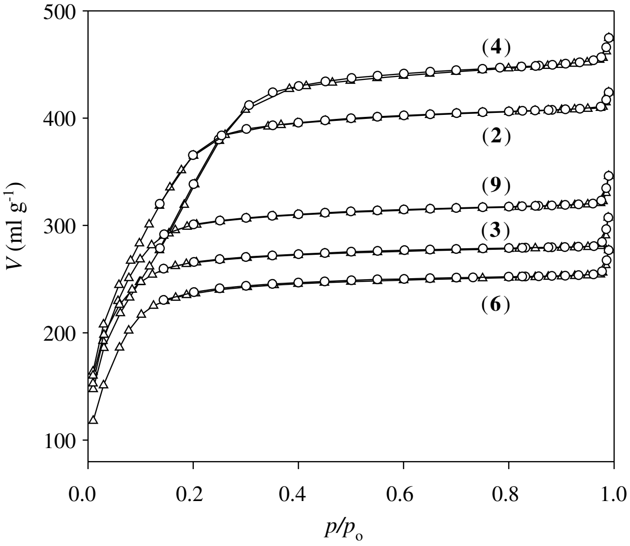

Fig. 3. N_2 adsorption (△) and desorption (○) isotherms for some ordered silicas templated with gemini surfactants calcined at 600 °C. See Tables 1 and 2 for captions.

All solids possess a high specific surface area, particularly those synthesized in an acidic medium (Tables 1 and 2). Surfactant 10–2–10 yielded materials with lower surface area, thus corroborating their poorer quality. The N_2 adsorption–desorption isotherms are of the type I (or intermediate between type I and type IV) with the step at a relative pressure around 0.2 for most of the solids (Fig. 3). These isotherms are typical of pores of sizes between the micro and meso ranges [29]. An increased pore volume and a step shifted toward higher relative pressure are observed for solids **2** and **4**. The large uptake at low partial pressures, particularly for **4** is due to the monolayer coverage of the mesopores and the increase in the adsorbed volume up to relative pressures of about 0.4 is accounted for by the filling of the mesopores [30]. The average pore diameter and the pore size distribution (Tables 1 and 2) confirmed the presence of pores in the upper limit micropore range. Fig. 4 depictes the pore size distributions of some materials determined by the BJH method. Although the applicability of the BJH method to this pore range is questionable, at least it can provide values for comparative purposes among the different materials. Moreover, it should be considered that the application of the BJH method can lead to an underestimation of the pore diameter [31]. As can be seen, all solids exhibited a narrow range of pore sizes. The pore size distributions of those materials synthesized in presence of gemini surfactant 10–2–10 (**3** and **7**) are even shifted to smaller pore sizes. Thus, the pore sizes for materials with similar structures, such as **2**, **3** and **4**, are directly related to the chain lengths of the gemini surfactants used as templates, which increase in the order: 8–2–16 > 12–2–12 > 10–2–10. On the other hand, the higher specific surface area and larger pore diameter and pore volume of those materials synthesized under acidic conditions (e.g., **4** vs. **9** or **2** vs. **6**) could be explained in terms of their synthesis mechanism, $S^+X^-I^+$, involving the mediation of halide counteranions X^-, which form an electrical double layer (S^+X^-)

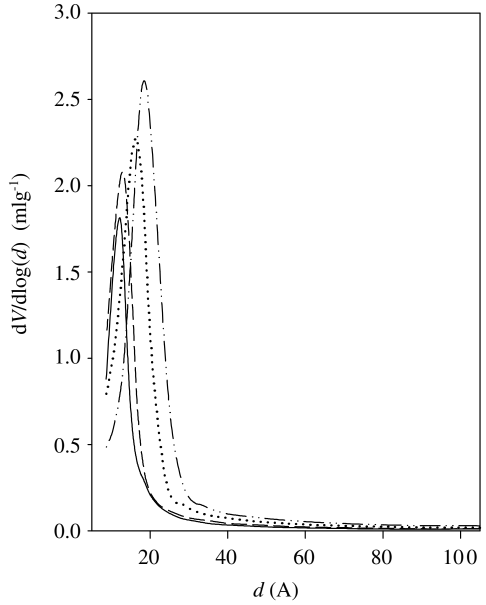

Fig. 4. Pore size distribution for some calcined ordered silicas: **2** (· · ·), **4** (- ·· -), **6** (—) and **9** (- - -). See Tables 1 and 2 for captions.

and serve to buffer the repulsion between [$\equiv$Si$(OH_2)^+$] (I^+) species and S^+ by means of weak hydrogen-bonding interactions [32,33].

The range of pore sizes estimated for all these materials is corroborated by those found in the literature for structurally similar materials. Thus, the cubic lattice parameter of an MCM-48 material with $d = 26$ Å is 77 Å [11], whereas that of the cubic faujasite (FAU) with $d = 7.4$ Å is 24.59 Å [30]. In the case of hexagonal structures, an MCM-41 mesophase with $a = 31.2$ Å has $d = 18$ Å [3], being the unit cell for the hexagonal faujasite (EMT) of 17.35 Å, with elliptical pores of 7.4×6.9 Å [30].

The wall thickness of the hexagonal ordered silicas was determined as the difference between the *a* parameter and the pore diameter (Tables 1 and 2). It was found to be in the range of 6–11 Å, irrespective of the synthesis conditions used. It should be noted the smaller pore wall thickness of those materials obtained by using surfactant 10–2–10 as template, which also accounts for the lower quality of these materials. For the cubic structure (**6**) (Table 2), it was calculated according to the formula given by Ravikovitch and coworkers [34]: pore wall thickness $= (a/3.092) - (d/2)$. These values are similar to those found for similar materials synthesized under very different conditions [15,32,33], thus confirming the range of pore sizes previously discussed.

4. Conclusion

Our results suggest that ordered porous silicas with pores in the micro–meso range can be synthesized by using assemblies of gemini surfactants as templates. Depending on the surfactant and reaction conditions, a variety of phases can be obtained. Under acidic conditions, only hexagonal phases resulted. However, under basic conditions, surfactant 12–2–12 produced an MCM-48 material, whereas surfactant 8–2–16 yielded MCM-41, both of a high quality. These results also illustrate that not only the overall hydrocarbon content but also the dissymmetry of the surfactants determine their mesophases in the presence of silica, and consequently the inorganic structures obtained. The mechanisms of formation of the different mesophases have been discussed in terms of the surfactant packing parameter and synthesis conditions.

Acknowledgements

F.J.R. and C.J. would like to thank Spain's Dirección General de Investigación, Ministry of Science and Technology, for funding this research within the framework of Project BQU2001-2605, Fondos Feder and Junta de Andalucía for additional financial support. This work was also supported by the CNRS, the University of Bordeaux I and the Région Aquitaine.

References

[1] A. Corma, Chem. Rev. 97 (1997) 2373.
[2] F. Marlow, M.D. McGehee, D. Zhao, B.F. Chmelka, G.D. Stucky, Adv. Mater. 11 (1999) 632.
[3] J.S. Beck, J.C. Vartuli, W.J. Roth, M.E. Leonowicz, C.T. Kresge, K.D. Schmitt, C.T.-W. Chu, D.H. Olson, E.W. Sheppard, S.B. McCullen, J.B. Higgins, J.L. Schlenker, J. Am. Chem. Soc. 114 (1992) 10834.
[4] C. Göltner, M. Antonietti, Adv. Mater. 9 (1997) 431.
[5] U. Ciesla, F. Schüth, Micropor. Mesopor. Mater. 27 (1999) 131.
[6] Q. Huo, D.I. Margolese, U. Ciesla, P. Feng, T.E. Gier, P. Sieger, R. Leon, P.M. Petroff, F. Schüth, G.D. Stucky, Nature 368 (1994) 317.
[7] P.T. Tanev, T.J. Pinnavaia, Science 267 (1995) 865.
[8] Q. Huo, R. Leon, P.M. Petroff, G.D. Stucky, Science 268 (1995) 1324.
[9] Q. Huo, D.I. Margolese, G.D. Stucky, Chem. Mater. 8 (1996) 1147.
[10] P. Van Der Voort, M. Mathieu, F. Mees, E.F. Vansant, J. Phys. Chem. B 102 (1998) 8847.
[11] O. Collart, P. Van Der Voort, E.F. Vansant, D. Desplantier, A. Galarneau, F. Di Renzo, F. Fajula, J. Phys. Chem. B 105 (2001) 12771.
[12] M. Benjelloun, P. Van Der Voort, P. Cool, O. Collart, E.F. Vansant, Phys. Chem. Chem. Phys. 3 (2001) 127.
[13] H.M.A. Hunter, P.A. Wright, Micropor. Mesopor. Mater. 43 (2001) 361.
[14] H.M.A. Hunter, A.E. García-Bennett, I.J. Shannon, W. Zhou, P.A. Wright, J. Mater. Chem. 12 (2002) 20.
[15] A.E. García-Bennett, S. Williamson, P.A. Wright, I.J. Shannon, J. Mater. Chem. 12 (2002) 3533.
[16] Z. Zhang, B. Tian, S. Shen, J. Fan, B. Tu, Q. Kong, F. Xiao, S. Qiu, D. Zhao, Chem. Lett. (2002) 584.

[17] R. Oda, I. Huc, S.J. Candau, Chem. Commun. (1997) 2105.
[18] R. Oda, I. Huc, J.-C. Homo, B. Heinrich, M. Schmutz, S. Candau, Langmuir 15 (1999) 2384.
[19] R. Oda, I. Huc, S.J. Candau, Angew. Chem. Int. Ed. 37 (1998) 2689.
[20] K. Sugiyasu, S. Tamaru, M. Takeuchi, D. Berthier, I. Huc, R. Oda, S. Shinkai, Chem. Commun. (2002) 1212.
[21] J.Y. Ying, C.P. Mehnert, M.S. Wong, Angew. Chem. Int. Ed. 38 (1999) 56.
[22] A.C. Voetglin, A. Matijasic, J. Patarin, C. Sauerland, Y. Grillet, L. Huve, Micropor. Mater. 10 (1997) 137.
[23] J.N. Israelachvili, D.J. Mitchell, B.W. Ninham, J. Chem. Soc., Faraday Trans. II 72 (1976) 1527.
[24] G.D. Stucky, A. Monnier, F. Schüth, Q. Huo, D. Margolese, D. Kumar, M. Krishnamurty, P. Petroff, A. Firouzi, M. Janicke, B.F. Chmelka, Mol. Cryst. Liq. Cryst. 240 (1994) 187.
[25] Q. Huo, D.I. Margolese, U. Ciesla, D.G. Demuth, P. Feng, T.E. Gier, P. Sieger, A. Firouzi, B.F. Chmelka, F. Schüth, G.D. Stucky, Chem. Mater. 6 (1994) 1176.
[26] A. Firouzi, A. Monnier, L.M. Bull, T. Besier, P. Sieger, Q. Huo, S.A. Walker, J.A. Zasadzinski, C. Glinka, J. Nicol, D. Margolese, G.D. Stucky, B.F. Chmelka, Science 267 (1995) 1138.
[27] J.-H. Sun, M.-O. Coppens, J. Mater. Chem. 12 (2002) 3016.
[28] C.A. Fyfe, G. Fu, J. Am. Chem. Soc. 117 (1995) 9709.
[29] U. Ciesla, S. Schacht, G.D. Stucky, K.K. Unger, F. Schüth, Angew. Chem., Int. Ed. Engl. 35 (1996) 541.
[30] C.-Y. Chen, H.-X. Li, M.E. Davis, Micropor. Mater. 2 (1993) 17.
[31] M. Kruk, M. Jaroniec, A. Sayari, Langmuir 13 (1997) 6267.
[32] A. Sayari, Stud. Surf. Sci. Catal. 102 (1996) 1.
[33] S. Biz, M.L. Occelli, Catal. Rev.—Sci. Eng. 40 (1998) 329.
[34] K. Schumacher, P.I. Ravikovitch, A. Du Chesne, A.V. Neimark, K.K. Unger, Langmuir 16 (2000) 4648.